BIOCHEMISTRY
including biophysical chemistry & molecular biology

Article

pubs.acs.org/biochemistry

# Structural Insight into Substrate Selectivity of *Erwinia chrysanthemi* L-Asparaginase

Hien Anh Nguyen,[†,‡] Ying Su,[†,‡] and Arnon Lavie*[,†,‡]

[†]The Jesse Brown VA Medical Center, Chicago, Illinois 60607, United States

[‡]Department of Biochemistry and Molecular Genetics, University of Illinois at Chicago, Chicago, Illinois 60607, United States

Supporting Information

**ABSTRACT:** L-Asparaginases of bacterial origin are a mainstay of acute lymphoblastic leukemia treatment. The mechanism of action of these enzyme drugs is associated with their capacity to deplete the amino acid L-asparagine from the blood. However, clinical use of bacterial L-asparaginases is complicated by their dual L-asparaginase and L-glutaminase activities. The latter, even though representing only ∼10% of the overall activity, is partially responsible for the observed toxic side effects. Hence, L-asparaginases devoid of L-glutaminase activity hold potential as safer drugs. Understanding the key determinants of L-asparaginase substrate specificity is a prerequisite step toward the development of enzyme variants with reduced toxicity. Here we present crystal structures of the *Erwinia chrysanthemi* L-asparaginase in complex with L-aspartic acid and with L-glutamic acid. These structures reveal two enzyme conformations—open and closed—corresponding to the inactive and active states, respectively. The binding of ligands induces the positioning of the catalytic Thr15 into its active conformation, which in turn allows for the ordering and closure of the flexible N-terminal loop. Notably, L-aspartic acid is more efficient than L-glutamic acid in inducing the active positioning of Thr15. Structural elements explaining the preference of the enzyme for L-asparagine over L-glutamine are discussed with guidance to the future development of more specific L-asparaginases.

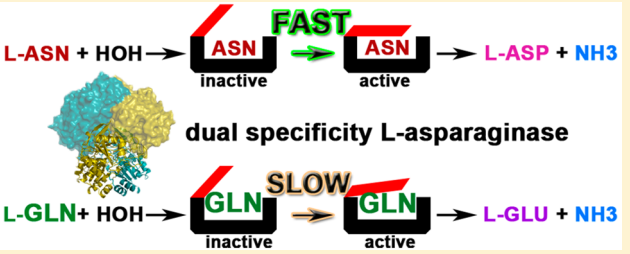


Bacterial L-asparaginases, specifically those from *Escherichia coli* and *Erwinia chrysanthemi*, are FDA-approved to treat certain blood cancers.[1] These enzyme drugs act to deplete the amino acid L-asparagine (ASN) present in blood. While most human cells can synthesize ASN de novo using the enzyme asparagine synthetase (ASNS), cancer cells that have lost or have low expression of ASNS are dependent on scavenging the amino acid from the blood. Hence, administration of these bacterial L-asparaginases selectively kills those cancer cells that have lost/low expression of ASNS, as occurs in acute lymphoblastic leukemia (ALL).

Amino acid amidohydrolases are enzymes that catalyze the hydrolysis of ASN or L-glutamine (GLN) to generate L-aspartate (ASP) or L-glutamate (GLU), respectively (Figure 1). Bacterial amino acid amidohydrolases belong to two classes. The aforementioned *E. coli* and *E. chrysanthemi* enzymes belong to a class that is referred to as L-asparaginases, since these enzymes primarily hydrolyze the amino acid ASN and are characterized by relatively low L-glutaminase activity (for a review on L-asparaginases see[2]). For these particular L-asparaginases, the L-glutaminase activity is about 2−10% of their L-asparaginase activities.[3] In contrast, enzymes that belong to the second class of amino acid amidohydrolases, such as the *Pseudomonas* 7A glutaminase-asparaginase[4] and the *Acinetobacter glutaminasificans* glutaminase-asparaginase,[5] have comparable L-asparaginase and L-glutaminase activities. Structural and sequence homology connects these two classes of bacterial amidohydrolyases.[6]

Following the discovery of the clinical potential of L-asparagine depletion,[7] enzymes from both classes of amino acid amidohydrolases were tested for their suitability as anticancer drugs. While both classes of enzymes showed toxic side effects, these were more pronounced for the enzymes with high L-glutaminase activity.[8−11] As a result, only enzymes that belong to the L-asparaginase class of amino acid amidohydrolases have made it into the clinic.[1] However, even for these low L-glutaminase enzymes, toxicity is still a challenge. Since toxicity of treatment with L-asparaginases has been correlated with the residual L-glutaminase activity of these enzyme drugs, it is not surprising that research toward the discovery or generation of more selective L-asparaginases has been conducted.[12−16] One factor that would greatly aid the rational design of low L-glutaminase L-asparaginase variants is detailed understanding of the molecular basis that governs the selectivity between ASN and GLN. To our knowledge, the most detailed analysis of this factor has been described by Aghaiypour et al. in 2001[17] for the *E. chrysanthemi* L-asparaginase (*ErA* hereafter). In that study, the crystal structure of *ErA* in complex with GLU was reported and compared to the previously reported *ErA* complex with

**Received:** December 15, 2015
**Revised:** February 5, 2016
**Published:** February 8, 2016

  

DOI: 10.1021/acs.biochem.5b01351
*Biochemistry* 2016, 55, 1246−1253

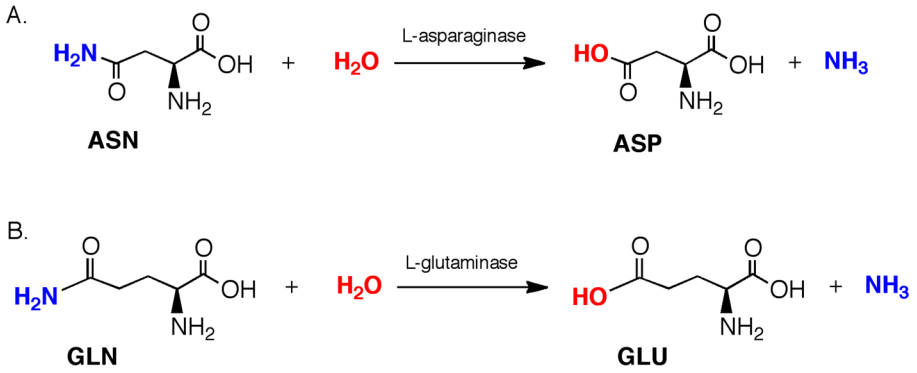


**Figure 1.** The L-asparaginase and L-glutaminase reactions. The *E. chrysanthemi* L-asparaginase has dual L-asparaginase and L-glutaminase activities. (A) The L-asparaginase reaction. (B) The L-glutaminase reaction.

ASP.[18] However, the coordinates of the *ErA* in complex with L-ASP have not been deposited in the Protein Data Bank (PDB), denying us the opportunity to inspect that model (a model of *ErA* in complex with D-ASP does exist, PDB ID 1HG1[17]). Moreover, the crystals used to solve the ASP and GLU complexes were first cross-linked and then soaked at pH 5.5 with the ligands.[17,18] Since low pH is known to promote the binding of ASP to the enzyme,[19] we reasoned the crystal structures of the complexes solved at physiological pH, and without crystal cross-linking, would better represent the true structure.

To elucidate the determinants of ASN and GLN selectivity of the *Erwinia* L-asparaginase, we determined the high-resolution crystal structures of this enzyme in complex with ASP and GLU (at 1.63 and 1.70 Å resolution, respectively). Both structures reported here are from crystals grown at pH 7.5 using the same crystallization conditions, not cross-linked, soaked with ligands at pH 7.5, have the identical space group and very similar unit cell parameters (see Experimental Procedures and Table 1). This allows us to minimize experimental artifacts when analyzing the observed differences between the structures of the complexes. Analysis of these *Erwinia* L-asparaginase structures reveals the molecular basis for GLN being an inferior substrate to ASN. This understanding can inform the design of variants that have increased selectivity against GLN while maintaining ASN as a substrate. Such low/no L-glutaminase variants of the *Erwinia* L-asparaginase are predicted to have reduced toxicity and may therefore have improved clinical utility.

## EXPERIMENTAL PROCEDURES

**Gene Cloning and Mutagenesis.** A codon-optimized synthetic gene corresponding to the amino acid sequence of *ErA* (UniProt entry P06608) lacking the first 22-amino acid signal peptide was synthesized by Genscript as described by Schalk et al.[20] The synthetic gene was digested with NdeI and *Bam*HI-HF restriction enzymes, gel purified, and ligated into a $His_6$-SUMO-pET14b vector (where the $His_6$ tag is followed by the yeast protein SUMO (small ubiquitin modifier, Smt3p) using Instant Sticky End DNA ligase (New England Biolabs), generating a $His_6$-SUMO-*ErA* plasmid.

**Protein Expression and Purification.** Protein expression and purification were performed as previously described.[20] In brief, the $His_6$-SUMO-*ErA* (residues 23−327) plasmid was transformed into *E. coli* BL21(DE3) C41 cells for expression. A single colony was selected and grown at 37 °C in 2xYT medium. Protein expression was induced with 0.3 mM isopropyl β-D-1-thiogalactopyranoside when the culture reached an optical density (at 600 nm) of 0.6−0.8. The incubation temperature was then reduced and maintained at 18 °C for the next 12 h. Protein was extracted from cells by sonication and cleared from debris by centrifugation at 20000*g*. The supernatant was loaded onto a 5 mL HisTrap nickel affinity column (GE Healthcare). The column was subsequently washed with buffers composed of 25 mM Tris-HCl, pH 8.5, 500 mM NaCl, and 25, 50, and 75 mM imidazole. The bound protein was eluted with the same buffer but containing 500 mM imidazole. The N-terminal $His_6$-SUMO tag was cleaved by SUMO protease, and the protein solution was loaded back onto a nickel affinity column to separate the tag. The flow-through fraction containing the purified enzyme in 25 mM Tris, pH 8.5, 100 mM NaCl was concentrated to 20−40 mg/mL, aliquoted, flash frozen in liquid nitrogen, and stored at −80 °C.

**Crystallization, X-ray Data Collection, and Refinement.** Crystals of *ErA* were grown at 285 K using the hanging-drop vapor-diffusion method. Two microliters of *Erwinia* at 10 mg/mL was mixed with 1 μL of reservoir buffer solution. The reservoir solution consisted of 0.1 M HEPES pH 7.5 and 24% PEG MME 2000.

Prior to data collection, crystals were soaked for 5 min in 0.1 M HEPES, pH 7.5 and 24% of PEG MME 2000 solution containing either 10 mM L-aspartic acid (Sigma A6683) or 5 mM L-glutamic acid (Sigma 128420). Soaked crystals were then transferred to the same solutions, respectively, but supplemented with 25% glycerol for cryoprotection.

Diffraction data were collected at the Life Sciences Collaborative Access Team (LS-CAT) beamline 21-ID-F at Argonne National Laboratory. Data were processed with the XDS package.[21] Structures were determined by molecular replacement with MOLREP[22] using the atomic resolution structure (PDB entry 1O7J[23]) as a search model. Refinement was conducted using REFMAC[24] and Phenix,[25] and model building was performed using Coot.[26] Since protomer D of the *ErA*-GLU complex showed a dual conformation for Thr15 plus clear, albeit weak density for the N-terminal loop, we performed refinement of atom occupancies. This step revealed a strong correlation between the occupancy of elements of the closed state and those of the open state. Specifically, the occupancy of the closed and open Thr15 refined to 0.66 and 0.34, respectively; the N-terminal loop (i.e., closed state) refined to an average occupancy of 0.63; likewise, the occupancies of the ligand GLU refined to 0.61 (active conformation) and 0.39 (inactive conformation). On the


DOI: 10.1021/acs.biochem.5b01351
*Biochemistry* 2016, 55, 1246−1253

Table 1. Data Collection and Refinement Statistics

| Structure | *ErA* + ASP | *ErA* + GLU |
|---|---|---|
| PDB codes | 5F52 | 5HW0 |
| **Data collection statistics** | | |
| X-ray source and detector | LS-CAT ID-F | |
| MARCCD 225 | LS-CAT ID-F | |
| MARCCD 225 | | |
| wavelength (Å) | 0.97872 | 0.97872 |
| temperature (K) | 100 | 100 |
| resolution[a] (Å) | 1.63 (1.73−1.63) | 1.70 (1.80−1.70) |
| number of reflections[b] | | |
| observed | 1096036 (165084) | 949527 (142868) |
| unique | 151130 (23795) | 128606 (19833) |
| completeness (%)[b] | 99.7 (98.3) | 99.3 (96.0) |
| $R_{sym}$ (%)[b] | 10.4 (71.9) | 8.1 (79.5) |
| CC(1/2)[b] | 99.8 (81.8) | 99.9 (79.6) |
| average $I/\sigma(I)$[b] | 15.65 (2.92) | 19.62 (2.55) |
| space group | $P2_12_12_1$ | $P2_12_12_1$ |
| unit cell (Å): *a*, *b*, *c* | 77.893 88.234 176.103 | 75.061 88.408 174.306 |
| Wilson B-factor (Å$^2$)[b] | 23.0 | 23.4 |
| **Refinement statistics** | | |
| refinement program | REFMAC5 | REFMAC5, PHENIX |
| $R_{cryst}$ (%) | 15.58 | 16.65 |
| $R_{free}$ (%) | 18.72 | 20.54 |
| resolution range (Å) | 30.0−1.6 | 30.0−1.7 |
| protein molecules per a.u. | 4 | 4 |
| number of atoms: | | |
| protein (ProtA, protB, protC, protD) | 2507, 2504, 2483, 2499 | 2412, 2392, 2399, 2493 |
| water molecules | 1175 | 1022 |
| PEG molecules | 5 | 0 |
| Asp molecules | 4 | |
| Glu molecules | | 4 |
| R.m.s. deviation from ideal: | | |
| bond length (Å) | 0.019 | 0.015 |
| bond angles (deg) | 1.8 | 1.5 |
| average B-factors (Å$^2$) | | |
| protein (ProtA, protB, protC, protD) | 16.7, 17.2, 17.5, 16.8 | 21.7, 17.0, 18.5, 17.5 |
| water molecules | 29.0 | 28.3 |
| Asp molecules | 16.0, 18.2, 17.4, 18.0 | |
| Glu molecules | | 26.2, 23.1, 22.7, 25.6 |
| Ramachandran plot statistics (%) | | |
| most favored regions | 96.88 | 97.50 |
| additionally allowed regions | 2.80 | 2.16 |
| outlier regions | 0.32 | 0.33 |

[a]High resolution shell in parentheses. [b]Taken from CORRECT.LP file after data reduction with XDS package.

basis of these numbers, we elected to set the occupancy values of the closed (active) state atoms to 0.67, and those of the open (inactive) to 0.33, reflecting an approximate 2:1 ratio of closed-to-open conformation in protomer D.

Data collection and refinement statistics are listed in Table 1. Structural figures were prepared using the PyMOL Molecular Graphics System (version 1.6.0, Schrödinger).

## RESULTS

**Similarities and Notable Differences between the *Erwinia* ASP and GLU Complex Structures.** As discussed above, the *E. chrysanthemi* L-asparaginase has both L-asparaginase and L-glutaminase activities, the latter being about 10% of the former.[3] To understand what intrinsic factors of this enzyme tilt the balance away from the L-glutaminase reaction, we solved the crystal structures of the ASP (*ErA*-ASP) and GLU (*ErA*-GLU) complexes, which represent the state of the products of the L-asparaginase and L-glutaminase reaction, respectively. *Erwinia* L-asparaginase, like most bacterial amino acid amidohydrolases, is a tetramer built by a dimer-of-dimers with 327 residues per protomer. The rmsd between the entire tetramer of the ASP complex and that of the GLU complex is 0.165 Å over 1075 atoms (Figure 2A). Hence, the overall fold is insensitive to the nature of the ligand. For each individual complex, the four protomers that build each tetramer are essentially identical; rmsd of ∼0.07 Å for the *ErA*-ASP complex protomers and ∼0.11 Å for the *ErA*-GLU complex protomers (over 270−300 atoms), Figure 2B,C. The overall equivalency of the protomers was also observed in the atomic resolution of this enzyme.[23]

However, there are significant local differences between the *ErA*-ASP and *ErA*-GLU complexes, the most notable being the conformation of the flexible N-terminal loop (residues 18−34). In previous structures of ligand-free L-asparaginases, this loop had no clear electron density.[20,27,28] However, in the presence of ligand the loop becomes ordered and is observed to close on the active site.[20] For the *ErA*-ASP complex, this N-terminal loop is clearly visible and identical in all four protomers (Figure 2B, zoom). This is not the case for the *ErA*-GLU complex, where we could model this loop in only one of the four protomers (Figure 2C, zoom). The disparity between the ability of the substrates to stabilize the flexible N-terminal loop was previously noted by others.[17] In the following sections we analyze the structures to gain insight into the contrasting ability of ASP and GLU to efficiently induce the stable, closed conformation of this N-terminal loop.

**Binding of ASP Induces Enzyme Closure and the Critical Productive Positioning of Thr15.** Electron density indicated, without ambiguity, the presence of the soaked ASP molecule at each of the four active sites present in the asymmetric unit and the orientation of the conserved Thr15 (Figure 3A,B and Supplementary Figure S1). Because of the equivalency of the protomers, the following discussion deals with protomer A but applies equally to all protomers. In the *ErA*-ASP complex, the side chain of the reaction product is observed sandwiched between the active site conserved threonines, Thr15 and Thr95 (Figure 3C). Thr95, in addition to Asp96 and Lys168, are conserved residues located on the same face of the ligand. Thr15, located on the opposite face, stabilizes the closed conformation of the N-terminal loop by forming a water-mediated interaction with the side chain of Tyr29. Finally, Glu63 interacts with the α-amino group of the ligand. We interpret the *ErA*-ASP complex structure as representing the active state of the enzyme, since the N-terminal loop is ordered and has closed on the active site, and most importantly, Thr15 is in proximity to the side chain of the substrate.

**Binding of GLU Largely Fails to Induce Enzyme Closure and Productive Positioning of Thr15.** In contrast to the *ErA*-ASP complex, protomers A, B, and C of the *ErA*-GLU complex (but not protomer D, see below) lacked observable electron density for the flexible N-terminal loop. This is despite the binding of GLU, which had clear electron density (Figure 4A and Supplementary Figure S2). Additionally, while in these three protomers Thr15 showed clear


DOI: 10.1021/acs.biochem.5b01351
*Biochemistry* 2016, 55, 1246−1253

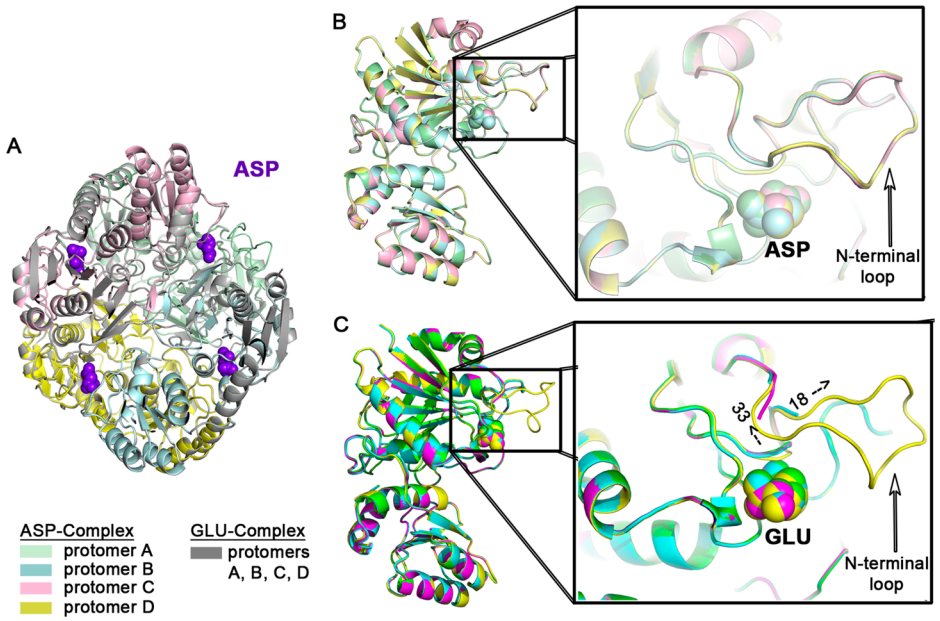


**Figure 2.** Binding of ASP versus GLU has no differential effect on the overall *Erwinia* L-asparaginase structure, whereas the ordering of the flexible N-terminal loop is sensitive to the nature of the amino acid ligand. (A) Overlay of the *ErA*-ASP complex tetramer (each protomer colored differently) and the *ErA*-GLU complex tetramer (all protomers colored gray) shows an identical overall fold. ASP molecules (purple) from the *ErA*-ASP complex indicate the location of the four active sites. (B) Overlay of the four individual protomers of the *ErA*-ASP complex reveals identical protomers with a bound ASP molecule at each active site, and a fully ordered N-terminal loop in all protomers (zoom). (C) Overlay of the four protomers of the *ErA*-GLU complex (colored as *ErA*-ASP but using brighter colors) reveals mostly identical protomers with a bound GLU molecule at each active site, but differences in the N-terminal loop. Three protomers (A, B, and C) had no electron density for this flexible loop, whereas for protomer D we could model the loop (zoom). The boundaries of the flexible N-terminal loop are marked with the beginning (18) and ending (33) residue numbers for this region.

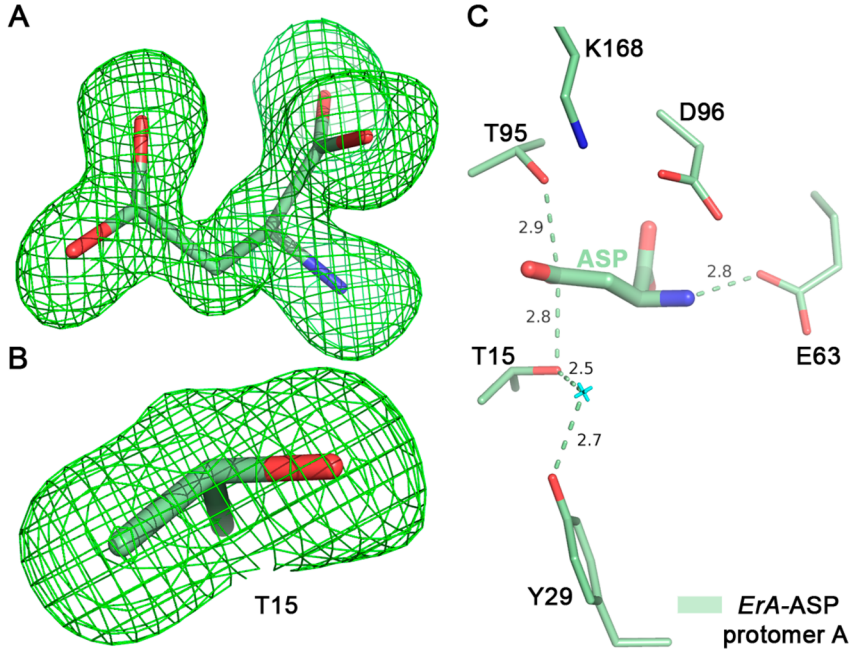


**Figure 3.** ASP binding mode to *ErA*. (A) Omit density for the ligand ASP in protomer A. (B) Omit density for the Thr15 in protomer A. Map used in A and B is a simulated annealing omit map, contoured at 2.5$\sigma$, where the ligand ASP was not included in the model, and Thr15 was mutated to a glycine, for the simulated annealing step (C) Binding of ASP to *ErA*: polar interactions between ASP and active site residues are indicated with dashed lines, with distances in angstroms. Note the water-mediated interaction between Tyr29, a residue located in the N-terminal loop, and the conserved Thr15.

electron density (Figure 4B and Supplementary Figure S2), this critical residue adopted a different conformation compared to that in the *ErA*-ASP complex (Figure 4C). Specifically, Thr15 in these protomers is rotated and positioned further away from the ligand (4.8 Å versus 2.8 Å) relative to its orientation in the *ErA*-ASP complex structure (gray circle, Figure 4C). We



DOI: 10.1021/acs.biochem.5b01351
*Biochemistry* 2016, 55, 1246−1253

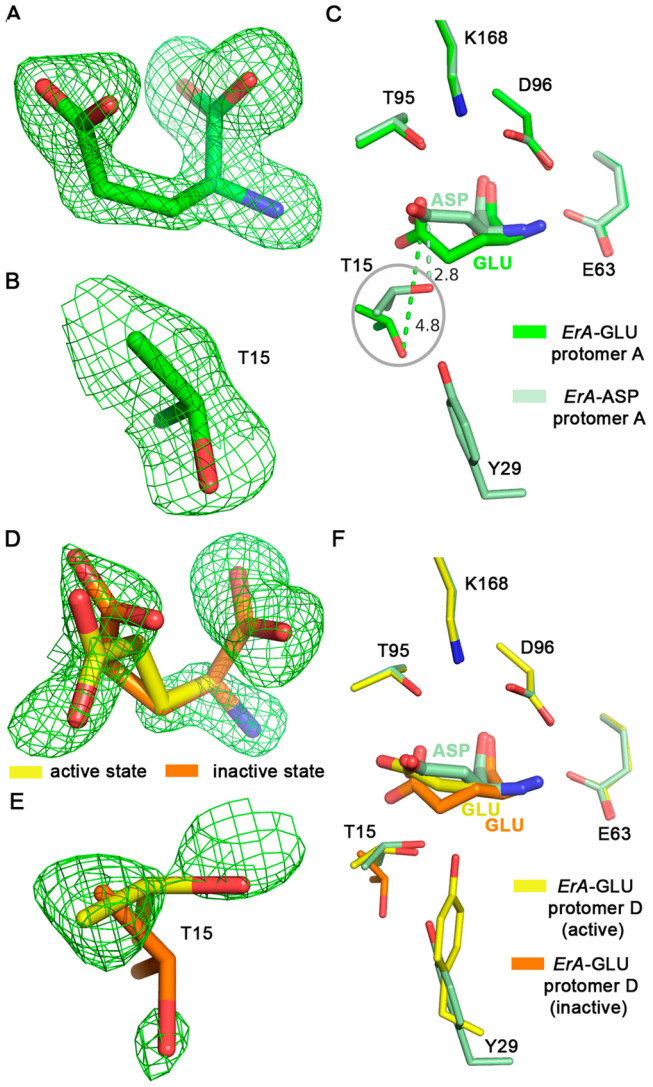


**Figure 4.** GLU binding mode to *ErA*. (A) Omit density for the ligand GLU in protomer A. (B) Omit density for the Thr15 in protomer A. (C) Overlay of the *ErA*-ASP (pale green) with the *ErA*-GLU protomer A (bright green). The N-terminal loop was not visible in the *ErA*-GLU protomer, and Thr15 is displaced and rotated relative to its position in the *ErA*-ASP structure (gray circle). (D) Omit density for the ligand GLU in protomer D. (E) Omit density for the Thr15 in protomer D. (F) Overlay of the *ErA*-ASP (pale green) with the *ErA*-GLU protomer D (orange, open conformation; yellow, closed conformation). We interpret the electron density for the GLU and Thr15 to represent two conformations. At 1/3 occupancy (orange), is the open state as seen in the other protomers of the *ErA*-GLU structure. At 2/3 occupancy (yellow), is the closed state, which resembles the closed state of the *ErA*-ASP structure. Map used in (A), (B), (D), and (E) is a simulated annealing omit map, contoured at 2.5$\sigma$, where the ligand GLU was not included in the model, and Thr15 was mutated to a glycine, for the simulated annealing step.

interpret the structure observed in these *ErA*-GLU protomers to represent an inactive state of the enzyme, presumably the state just after the binding of the substrate GLN. The *ErA* conformation and the position of the ligand GLU in these three protomers of our *ErA*-GLU complex are very similar to that previously observed for all four protomers by Aghaiypour et al. in their analogous complex (PDB ID 1HFW).[17]

In contrast, the electron density of protomer D of the *ErA*-GLU complex is consistent with a dual conformation for the bound GLU and for Thr15 (Figure 4D,E). Significantly, in protomer D we observed weak but unambiguous electron density for the closed N-terminal loop (Supplementary Figure S3). Analysis of the refined occupancies for the ligand, Thr15, and the N-terminal loop suggest a 1:2 ratio between two distinct states. One state, approximated at 1/3 occupancy, is very similar to the state observed in protomers A, B, and C discussed earlier—that is, the open/inactive state (depicted in orange, Figure 4D–F). The second state, estimated at 2/3 occupancy (see Experimental Procedures for how occupancy was determined), reveals the GLU and Thr15 in a conformation approaching that seen in the closed/active *ErA*-ASP structure (yellow, Figure 4D–F). In this second state we correlated correct positioning of GLU to closure of the N-terminal loop. The comparatively weak electron density for the N-terminal loop of protomer D is not surprising based on its partial occupancy coupled with the intrinsic flexibility of this loop. Of note, while binding of GLU induced the closure of this loop, residue Tyr29 adopts a slightly different conformation relative to the one seen in the *ErA*-ASP complex structure (Figure 4F). This is likely due to the incomplete rotation of Thr15 to its active conformation as seen in the presence of ASP. Nevertheless, we interpret the closed component of the structure of protomer D as representing the active GLU-bound conformation, whereas the open component represents the inactive state (as observed in the other protomers).

## DISCUSSION

**Coupling Ligand Binding to N-Terminal Loop Closure via Thr15.** Our structures suggest that GLN is a worse substrate than ASN as it is not efficient in promoting the active enzyme conformation. Specifically, GLN is less efficient in inducing the rotation of Thr15 to its active conformation, which in turn is required for initiating the closure of the flexible N-terminal loop. This interplay between Thr15 adopting its active conformation and N-terminal loop closure is likely to be a general feature of this type of L-asparaginases and showcases a novel mechanistic principle of these enzymes.

To understand the distinctive effect of ASN versus GLN on the enzyme conformation, we overlaid the *ErA*-ASP structure (closed conformation) on the *ErA*-GLU protomer A (open conformation) and protomer D (closed conformation fraction) structures with a focus on the N-terminal loop and select active site residues (Figure 5). Interestingly, the position of most active site residues is completely insensitive to the presence of ligand: irrespective of the ligand type, ASP or GLU, active site residues Glu63, Thr95, Asp96, and Lys168 occupy identical positions. Additionally, the state of the N-terminal loop (open versus closed) has no impact on the position of these residues.

The situation is very different at the opposite face of the ligand, the face toward Thr15 and Tyr29 (which is a part of the flexible N-terminal loop). We can identify three distinct enzyme states. In one extreme, as displayed by protomers A, B, and C of the *ErA*-GLU structure, the ligand is bound at the active site but has failed to induce the transition of Thr15 to its closed conformation (only protomer A shown for simplicity, bright green, Figure 5A). When modeling the N-terminal loop in the closed conformation known from the *ErA*-ASP structure, we measure a short (<3 Å) distance between Thr15 and the phenyl ring of Tyr29. Hence, Thr15 in its open conformation is not compatible with closure of the N-terminal loop, and this factor explains why we could not observe electron density for this loop in protomers A, B, and C of the *ErA*-GLU complex.


DOI: 10.1021/acs.biochem.5b01351
*Biochemistry* 2016, 55, 1246–1253

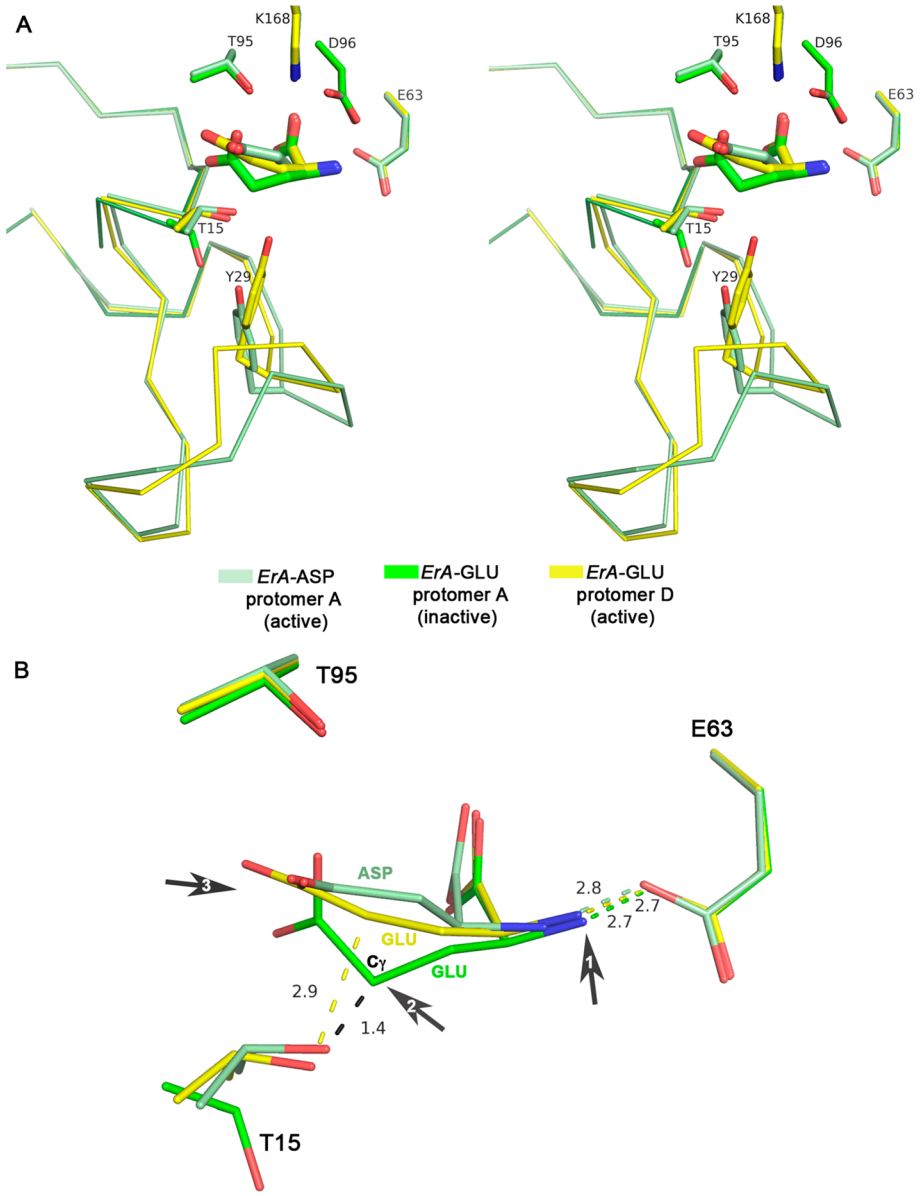


**Figure 5.** Thr15 couples substrate binding and closure of the N-terminal loop. (A) Stereoview showing an overlay of select regions from the *ErA*-ASP complex (pale green) and the *ErA*-GLU complex protomers A (bright green) and D (yellow). For the *ErA*-ASP complex, binding of ligand affects the conformation of Thr15, which in turn promotes closure of the N-terminal loop. In contrast, binding of GLU either did not (protomer A) or only partially (protomer D) induced this change to the Thr15 conformation. Note that the position of most active site residues (Glu63, Thr95, Asp96, and Lys168) is insensitive to the nature of the ligand (ASP versus GLU). In contrast, the conformation of Thr15 is sensitive to the type of ligand. Binding of ASP induces a conformational change in Thr15 that results in a state that is consistent with the closed N-terminal loop. Lacking this conformational change in Thr15, as seen in protomer A of the *ErA*-GLU structure, the methyl group of the Thr15 side chain would clash with Tyr29. In protomer D of the *ErA*-GLU structure, binding of GLU did induce a partial rotation of Thr15, which in turn allowed for N-terminal loop closure. (B) Conformation of ASP versus GLU in the *Erwinia* L-asparaginase active site. See text for details.

In the intermediate enzyme state, observed in protomer D of the *ErA*-GLU structure (the closed fraction, which is interpreted as the active state, shown in yellow, Figure 5A), ligand binding has partially induced Thr15 transition to a conformation nearing the closed state, and this allows the N-terminal loop to close. Finally, in the fully closed state, as observed in *ErA*-ASP, the Thr15 side chain has fully rotated into what we interpret as the active conformation. This rotation of Thr15 into the active conformation allows the flexible loop to close.

The rather significant change in Thr15 conformation between the open and closed states effects not only the side-chain of Thr15, but also the position of the main-chain. The residue prior to Thr15 is Gly14, a conserved residue in this family of L-asparaginases. The difference in main-chain atom positions between the closed (*ErA*-ASP) and open (*ErA*-GLU, protomer A) increases gradually from 0.4 Å at the Gly14 C$\alpha$ atom to a value of 1.0 Å at the Thr15 C$\alpha$ atom (Supplementary Figure S4). The movement of Thr15 between the open and closed states rationalizes the conservation of the preceding flexible glycine residue.

This analysis reveals the steps required for catalysis by L-asparaginases: binding of substrate, induction of the active Thr15 conformation, which in turn allows for the ordering and



DOI: 10.1021/acs.biochem.5b01351
*Biochemistry* 2016, 55, 1246−1253

closure of the flexible N-terminal loop. Why is the closure of this loop required for catalysis, despite the fact that it contains no essential residues? Note that mutation of Tyr29 (located in this loop) has only a moderate effect on the reaction rate.[29,30] One reason could be that closure of this loop is required for stabilizing Thr15 in the catalytically competent conformation. An additional reason could be that loop closure correctly positions active site water molecules that are required for catalysis.

**The Additional Methylene Group Present in GLN Sterically Prevents the Active Thr15 Conformation.** The above discussion lays out the differential effects of ASN (that promotes) and GLN (that hinders) on inducing Thr15 and the N-terminal loop of the *Erwinia* L-asparaginase into the active conformation. To shed light on the molecular reasons behind this difference, we inspected the binding mode of ASP and GLU to the enzyme. ASP fits seemingly without strain in the active site, with the side-chain carboxylic group being sandwiched between Thr15 and Thr95 (Figure 5B). To accommodate the additional methylene group that differentiates GLU from ASP, several adjustments to the GLU binding mode are required. First, the larger amino acid shifts ~0.7 Å toward Glu63, which in turn adjusts its side-chain position to maintain a 2.7−2.8 Å distance to the $\alpha$-amino group of GLU (arrow 1, Figure 5B). Second, to maintain a similar position to the side-chain carboxylic group as is present with ASP-bound, the GLU side-chain must bend, with the C$\gamma$ atom shifting toward Thr15 (arrow 2, Figure 5B). As a result, Thr15 is hindered from adopting the closed conformation, as the modeled distance between the closed Thr15 (as seen in the ASP complex) and the C$\gamma$ atom would be a repulsing 1.4 Å. Despite these two adjustments (seen in *ErA*-GLU protomers A, B, C, and with partial occupancy in D) at both extremities of the amino acid ligand, the side-chain still fails to properly position in the active site (arrow 3, Figure 5). Consequently, despite the contortions to fit the one-carbon longer GLU versus ASP, the positioning of the moiety where the hydrolytic reaction occurs is not optimal.

Yet, *ErA* does catalyze the hydrolysis of GLN. The question then becomes, how is productive positioning of GLN achieved? The active state of the *ErA*-GLU protomer D structure provides clues to this question. First, the GLU side-chain carboxylic acid moiety rotates to a conformation as seen for ASP, and this increases the separation between the C$\gamma$ atom and Thr15. Second, in response to the movement of the C$\gamma$ atom, Thr15 can rotate to its active state without steric hindrance (distance between Thr15 and the C$\gamma$ atom in this active state is an acceptable 2.9 Å, Figure 5B). Lastly, the adjustment of Thr15 allows for closure of the N-terminal loop, bringing the enzyme into its active state.

The N-terminal region of the *Erwinia* L-asparaginase is inherently mobile; it is not visible in crystal structures of this enzyme lacking a ligand,[20,27,28] and even when the preferred ligand ASP is bound, the B-factors of this region are higher relative to the other parts of the structure (Supplementary Figure S5). In the presence of the less preferred ligand GLU, the B-factors of the N-terminal loop are even higher, despite having average B-factor values very similar to the *ErA*-ASP complex in the remaining parts of the molecule. It is notable that the Wilson B-factors are very similar between the *ErA*-ASP and *ErA*-GLU data sets (Table 1). Hence, we can accurately compare the average B-factor values and conclude that the N-terminal loop of the GLU complex is less anchored relative to the ASP complex. The B-factor analysis underscores the reduced ability of GLU to stabilize the closed state and, together with the above observations, explains the reduction in the hydrolytic rate and increased Km of GLN versus ASN.

In summary, it is the differential ability between ASN (high) and GLN (low) to promote the active Thr15 conformation, and consequently the closed N-terminal loop, that is responsible for the enzyme's selectivity between these two substrates. One conclusion from this analysis is that in order to design variants that discriminate against GLN, one should introduce mutations that are not compatible with the closed enzyme state when GLN binds, but maintain compatibility with the closed state when ASN binds. Since GLN does bind slightly differently to ASN (Figure 5), it is conceptually possible to identify such mutations. As postulated by Aghaiypour et al.,[17] Glu63 and Ser254 are prime candidates for mutagenesis, as well as other sites (e.g., Ala31) that are predicted to be sensitive to the nature of the amino acid substrate.

## ■ ASSOCIATED CONTENT

### Supporting Information

The Supporting Information is available free of charge on the ACS Publications website at DOI: 10.1021/acs.biochem.5b01351.

Figure S1 presents omit maps for the ligands ASP and residue Thr15 of protomers B, C, and D of the *ErA*-ASP structure. Figure S2 presents omit maps for the ligands GLU and residue Thr15 of protomers B and C of the *ErA*-GLU structure. Figure S3 presents an omit map of the N-terminal loop of protomer D of the *ErA*-GLU structure. Figure S4 showcases the change in main-chain positions in the vicinity of Thr15 between the open and closed states of *ErA*. Figure S5 presents a plot of the average residue B-factor versus residue number for protomers D of the ASP and GLU complexes (PDF)

## ■ AUTHOR INFORMATION


### Corresponding Author

*Address: 900 South Ashland Avenue, MBRB room 1108, Chicago, IL, 60607. Phone: (312) 355-5029; Fax: (312) 355-4535. E-mail: Lavie@uic.edu.



### Funding

This work was supported in part by NIH Grant RO1 EB013685 and by Merit Review Award No. I01BX001919 from the United States (U.S.) Department of Veterans Affairs Biomedical Laboratory Research and Development Service. The contents do not represent the views of the U.S. Department of Veterans Affairs or the United States Government.


### Notes

The authors declare no competing financial interest.

## ■ ACKNOWLEDGMENTS


We would like to thank Dr. Amanda Schalk for much appreciated technical support as well as the staff at LS-CAT for their helpful assistance during data collection. We also thank Dr. Schalk for review of the manuscript.


## ■ ABBREVIATIONS

ASNS, asparagine synthetase; *ErA*, *Erwinia chrysanthemi* L-asparaginase; *ErA*-ASP, *Erwinia chrysanthemi* L-asparaginase



DOI: 10.1021/acs.biochem.5b01351
*Biochemistry* 2016, 55, 1246−1253

wild type in complex with ASP; *ErA*-GLU, *Erwinia chrysanthemi* L-asparaginase wild type in complex with GLU

## REFERENCES


(1) Asselin, B. L. (2011) L-asparaginase for treatment of childhood acute lymphoblastic leukemia: what have we learned? *Pediatr Blood Cancer 57*, 357−358.

(2) Michalska, K., and Jaskolski, M. (2006) Structural aspects of L-asparaginases, their friends and relations. *Acta Biochim Pol 53*, 627−640.

(3) Narta, U. K., Kanwar, S. S., and Azmi, W. (2007) Pharmacological and clinical evaluation of L-asparaginase in the treatment of leukemia. *Crit Rev. Oncol Hematol 61*, 208−221.

(4) Roberts, J. (1976) Purification and properties of a highly potent antitumor glutaminase-asparaginase from Pseudomonas 7Z. *J. Biol. Chem. 251*, 2119−2123.

(5) Steckel, J., Roberts, J., Philips, F. S., and Chou, T. C. (1983) Kinetic properties and inhibition of Acinetobacter glutaminase-asparaginase. *Biochem. Pharmacol. 32*, 971−977.

(6) Jakob, C. G., Lewinski, K., LaCount, M. W., Roberts, J., and Lebioda, L. (1997) Ion binding induces closed conformation in Pseudomonas 7A glutaminase-asparaginase (PGA): crystal structure of the PGA-SO4(2-)-NH4+ complex at 1.7 A resolution. *Biochemistry 36*, 923−931.

(7) Broome, J. D. (1963) Evidence that the L-asparaginase of guinea pig serum is responsible for its antilymphoma effects. I. Properties of the L-asparaginase of guinea pig serum in relation to those of the antilymphoma substance. *J. Exp. Med. 118*, 99−120.

(8) Warrell, R. P., Jr., Arlin, Z. A., Gee, T. S., Chou, T. C., Roberts, J., and Young, C. W. (1982) Clinical evaluation of succinylated Acinetobacter glutaminase-asparaginase in adult leukemia. *Cancer Treat Rep. 66*, 1479−1485.

(9) Distasio, J. A., Salazar, A. M., Nadji, M., and Durden, D. L. (1982) Glutaminase-free asparaginase from vibrio succinogenes: an anti-lymphoma enzyme lacking hepatotoxicity. *Int. J. Cancer 30*, 343−347.

(10) Reinert, R. B., Oberle, L. M., Wek, S. A., Bunpo, P., Wang, X. P., Mileva, I., Goodwin, L. O., Aldrich, C. J., Durden, D. L., McNurlan, M. A., Wek, R. C., and Anthony, T. G. (2006) Role of glutamine depletion in directing tissue-specific nutrient stress responses to L-asparaginase. *J. Biol. Chem. 281*, 31222−31233.

(11) Parmentier, J. H., Maggi, M., Tarasco, E., Scotti, C., Avramis, V. I., and Mittelman, S. D. (2015) Glutaminase activity determines cytotoxicity of L-asparaginases on most leukemia cell lines. *Leuk. Res. 39*, 757−762.

(12) Kumar, S., Venkata Dasu, V., and Pakshirajan, K. (2011) Purification and characterization of glutaminase-free L-asparaginase from Pectobacterium carotovorum MTCC 1428. *Bioresour. Technol. 102*, 2077−2082.

(13) Offman, M. N., Krol, M., Patel, N., Krishnan, S., Liu, J., Saha, V., and Bates, P. A. (2011) Rational engineering of L-asparaginase reveals importance of dual activity for cancer cell toxicity. *Blood 117*, 1614−1621.

(14) Derst, C., Henseling, J., and Rohm, K. H. (2000) Engineering the substrate specificity of Escherichia coli asparaginase. II. Selective reduction of glutaminase activity by amino acid replacements at position 248. *Protein Sci. 9*, 2009−2017.

(15) Ln, R., Doble, M., Rekha, V. P., and Pulicherla, K. K. (2011) In silico engineering of L-asparaginase to have reduced glutaminase side activity for effective treatment of acute lymphoblastic leukemia. *J. Pediatr. Hematol./Oncol. 33*, 617−621.

(16) Cappelletti, D., Chiarelli, L. R., Pasquetto, M. V., Stivala, S., Valentini, G., and Scotti, C. (2008) Helicobacter pyloril-asparaginase: a promising chemotherapeutic agent. *Biochem. Biophys. Res. Commun. 377*, 1222−1226.

(17) Aghaiypour, K., Wlodawer, A., and Lubkowski, J. (2001) Structural basis for the activity and substrate specificity of Erwinia chrysanthemi L-asparaginase. *Biochemistry 40*, 5655−5664.

(18) Miller, M., Rao, J. K., Wlodawer, A., and Gribskov, M. R. (1993) A left-handed crossover involved in amidohydrolase catalysis. Crystal structure of Erwinia chrysanthemi L-asparaginase with bound L-aspartate. *FEBS Lett. 328*, 275−279.

(19) Buchanan, G. R., and Holtkamp, C. A. (1980) Reduced antithrombin III levels during L-asparaginase therapy. *Med. Pediatr. Oncol. 8*, 7−14.

(20) Schalk, A. M., Nguyen, H. A., Rigouin, C., and Lavie, A. (2014) Identification and structural analysis of an L-asparaginase enzyme from guinea pig with putative tumor cell killing properties. *J. Biol. Chem. 289*, 33175−33186.

(21) Kabsch, W. (2010) Integration, scaling, space-group assignment and post-refinement. *Acta Crystallogr., Sect. D: Biol. Crystallogr. 66*, 133−144.

(22) Vagin, A., and Teplyakov, A. (1997) MOLREP: an automated program for molecular replacement. *J. Appl. Crystallogr. 30*, 1022−1025.

(23) Lubkowski, J., Dauter, M., Aghaiypour, K., Wlodawer, A., and Dauter, Z. (2003) Atomic resolution structure of Erwinia chrysanthemi L-asparaginase. *Acta Crystallogr., Sect. D: Biol. Crystallogr. 59*, 84−92.

(24) Murshudov, G. N., Vagin, A. A., and Dodson, E. J. (1997) Refinement of macromolecular structures by the maximum-likelihood method. *Acta Crystallogr., Sect. D: Biol. Crystallogr. 53*, 240−255.

(25) Adams, P. D., Afonine, P. V., Bunkoczi, G., Chen, V. B., Davis, I. W., Echols, N., Headd, J. J., Hung, L. W., Kapral, G. J., Grosse-Kunstleve, R. W., McCoy, A. J., Moriarty, N. W., Oeffner, R., Read, R. J., Richardson, D. C., Richardson, J. S., Terwilliger, T. C., and Zwart, P. H. (2010) PHENIX: a comprehensive Python-based system for macromolecular structure solution. *Acta Crystallogr., Sect. D: Biol. Crystallogr. 66*, 213−221.

(26) Emsley, P., Lohkamp, B., Scott, W. G., and Cowtan, K. (2010) Features and development of Coot. *Acta Crystallogr., Sect. D: Biol. Crystallogr. 66*, 486−501.

(27) Jaskolski, M., Kozak, M., Lubkowski, J., Palm, G., and Wlodawer, A. (2001) Structures of two highly homologous bacterial L-asparaginases: a case of enantiomorphic space groups. *Acta Crystallogr., Sect. D: Biol. Crystallogr. 57*, 369−377.

(28) Swain, A. L., Jaskolski, M., Housset, D., Rao, J. K., and Wlodawer, A. (1993) Crystal structure of Escherichia coli L-asparaginase, an enzyme used in cancer therapy. *Proc. Natl. Acad. Sci. U. S. A. 90*, 1474−1478.

(29) Derst, C., Wehner, A., Specht, V., and Rohm, K. H. (1994) States and functions of tyrosine residues in Escherichia coli asparaginase II. *Eur. J. Biochem. 224*, 533−540.

(30) Aung, H. P., Bocola, M., Schleper, S., and Rohm, K. H. (2000) Dynamics of a mobile loop at the active site of Escherichia coli asparaginase. *Biochim. Biophys. Acta, Protein Struct. Mol. Enzymol. 1481*, 349−359.




DOI: 10.1021/acs.biochem.5b01351
*Biochemistry* 2016, 55, 1246−1253